PHYSICAL REVIEW D **93,** 026007 (2016)

Holographic thermalization with initial long range correlation

Shu Lin*

Institute of Astronomy and Space Science, Sun Yat-Sen University, 135 Xingang Xi Road, Guangzhou, Guangdong 510275, China and RIKEN-BNL Research Center, Brookhaven National Laboratory, Upton, New York 11973, USA

(Received 5 December 2015; published 19 January 2016)

We studied the evolution of the Wightman correlator in a thermalizing state modeled by AdS_3-Vaidya background. We gave a prescription for calculating the Wightman correlator in coordinate space without using any approximation. For equal-time correlator $\langle O(v,x)O(v,0)\rangle$, we obtained an enhancement factor v^2 due to long range correlation present in the initial state. This was missed by previous studies based on geodesic approximation. We found that the long range correlation in initial state does not lead to significant modification to thermalization time as compared to known results with generic initial state. We also studied the spatially integrated Wightman correlator and showed evidence on the distinction between long distance and small momentum physics for an out-of-equilibrium state. We also calculated the radiation spectrum of particles weakly coupled to O and found that lower frequency mode approaches thermal spectrum faster than high frequency mode.

DOI: 10.1103/PhysRevD.93.026007

I. INTRODUCTION AND SUMMARY

The phenomenon of thermalization, where a quantum field state evolves unitarily from a pure state to an apparent thermal state, exists in many different areas of physics, including heavy ion collisions, the cold atom system etc. Since systems having the thermalization phenomenon are usually strongly coupled, theoretical studies of thermalization remain a difficult task. The application of gauge/gravity duality allows us to study dynamics of strongly coupled field theory by solving weakly coupled gravity in one dimension higher, providing a useful alternative to traditional methods. Recently, there has been significant progress in understanding thermalization using the holographic method.

Useful probes of the thermalization process are correlation functions. These include local probes like the one-point function and nonlocal probes like the two-point function. They contain different information on the thermalization process. For example, in the context of heavy ion collisions, the one-point function of stress energy tensor determines the spectrum of hadron, which is emitted only at freeze-out, while the two-point function of electromagnetic current determines the spectrum of photon/dilepton, which is emitted throughout the history of quark gluon plasma evolution. The calculation of one-point functions, usually involving solving Einstein equations, has been pursued by many groups; see for example [9,11,12,14,17,20–24,34,35,37,38,43,48,49]. We focus on two-point functions in this work. The calculation of two-point functions, as pointed out in [16], depends on the order of operators. While the retarded correlator is independent of the field theory state, the Wightman correlator does depend on the state. Consequently, the former can be obtained by studying response of bulk field to external boundary source. On the contrary, the calculation of the latter must be formulated as an initial value problem, with the initial value encoding state information.

Previous studies on the two-point function used different approximation schemes, such as quasistatic approximation [2,3,10,25,26,36,42,46,47], geodesic approximation [1,4–8,13,33], geometric optics approximation [16,18,19,30–32,39] etc. Recently, a rigorous calculation has been done by Keränen and Kleinert (KK) for the Wightman correlator in (spatial) momentum space [41]; see also [27,29,40] for related attempts. In this work, we present results for the same correlator in coordinate space. For technical reasons, we focus on AdS_3 Vaidya or thermalization of $1+1$D conformal field theory (CFT). Our results in coordinate space allow for direct comparison to general CFT results by Calabrese and Cardy (CC) [15]. While CC assume finite correlation length in the initial state, our initial (vacuum) state contains long range correlation. Consequently our results are reminiscent of long range correlation: The equal-time correlator $\langle O(v,x)O(v,0)\rangle$ for a scalar operator O with dimension 2 has power law factor v^2/x^4 in the regime $x \gg v \gg 1$. Previous studies based on geodesic approximation captured the x-dependence, but missed the v-dependence. The general results of CC determine a thermalization time $x + O(1/T)$ for points with spatial separation x, and a thermalization time $O(1/T)$ for points with temporal separation δv. We confirmed that the conclusion is still true when initial state has long range correlation.

We have also studied the spatially integrated correlator, that is, the zero (spatial) momentum mode of the Wightman correlator. While low momentum mode is usually regarded as equivalent to long distance physics, we found a

*linshu8@mail.sysu.edu.cn

counterexample: when the state is far from equilibrium, the zero momentum correlator receives dominant contribution from integrating over the correlator with small separation, i.e. short distance physics. Furthermore, we calculate the spectrum of particles weakly coupled to operator O at different stages of thermalization. Our results indicate that high frequency modes tend to appear thermal slower than low frequency modes.

II. PROBING A THERMALIZATION PROCESS WITH THE WIGHTMAN CORRELATOR

We consider a thermalizing state modeled by AdS_3-Vaidya background below

$$ds^2 = \frac{-fdv^2 - 2dvdz + dx^2}{z^2}, \tag{1}$$

with $f = 1 - mz^2\theta(v)$. Here v is a light cone coordinate, which is related to usual coordinates t and z by

$$dv = dt - \int_0^z \frac{dz'}{f(z')}. \tag{2}$$

The metric corresponds to a lightlike shell (shock wave) collapsing from the boundary at $v = 0$. The hypersurface $v = 0$, $x =$ arbitrary separates empty anti–de Sitter (AdS) and Banados-Teitelboim-Zanelli (BTZ) metrics on different sides of the shell. Empty AdS and BTZ metrics are dual to vacuum and thermal CFT states respectively. The Vaidya background is dual to a thermalization process, triggered by an instantaneous injection of energy density to vacuum state at $t = 0$. The end point of the thermalization process is a thermal state with temperature $T = \sqrt{m}/2\pi$. We set $m = 1$ from now on. We choose to probe the thermalizing state by the Wightman correlator $\langle O(t,x)O(t',x')\rangle$. O is a dimension 2 scalar operator dual to bulk dilaton. Unlike the retarded correlator, the Wightman correlator cannot be calculated from the response of bulk field to source on the boundary. This is because the retarded correlator is state independent, while the Wightman correlator depends on the state. In [16], the calculation of the generic correlator was formulated as an initial value problem. The equivalence of the formulation with standard holographic dictionary was shown by KK [41], based on a more general prescription for real-time holography [44,45]. We use the formulation for our specific setup. The bulk Wightman correlator can be written as

$$G^>(4|3) = \int dz_1 dx_1 dz_2 dx_2 G_0^>(2|1) \times \overleftrightarrow{D}^{v1}\overleftrightarrow{D}^{v2} G^R_{\rm th}(3|1)G^R_{\rm th}(4|2), \tag{3}$$

where $iG_0^>(2|1) = \langle\hat{\phi}(v_2,x_2,z_2)\hat{\phi}(v_1,x_1,z_1)\rangle$ is the bulk Wightman correlator evaluated on the hypersurface of the shell $v_2 = v_1 = 0$. This is our initial value. Assuming the continuity of the bulk correlator across the shell, we can use the value of $G_0^>(2|1)$ in empty AdS. $iG^R_{\rm th}(3|1) = \langle[\hat{\phi}(v_3,x_3,z_3),\hat{\phi}(v_1,x_1,z_1)]\rangle\theta(t_3 - t_1)$ and $iG^R_{\rm th}(4|2)$ defined similarly are retarded bulk-bulk propagators in BTZ, which propagate points 1 and 2 from empty AdS to points 3 and 4 on the BTZ side. The resulting bulk correlator $G^>(4|3) = i\langle\hat{\phi}(v_4,x_4,z_4)\hat{\phi}(v_3,x_3,z_3)\rangle$ gives us the boundary Wightman correlator:

$$\langle G^>(4|3)\rangle \to z_4^2 z_3^2\langle O(v_4,x_4)O(v_3,x_3)\rangle, \quad \text{as } z_4, \quad z_3 \to 0. \tag{4}$$

The symbol $\overleftrightarrow{D}^v = \sqrt{-g}g^{vz}\overleftrightarrow{\partial}_z$ is a two-way differential operator. Note that it only involves derivative with respect to z. It means that we need only one initial value $G_0^>(2|1)$. This is in contrast to conventional initial value problems where we need both position and velocity. The reason is that we are using light cone coordinate v and our initial value hypersurface is also lightlike. The simplification comes with a price: The initial value $G_0^>(2|1)$ is singular as the points 2 and 1 approach the light cone. Nevertheless, we can eliminate the singularity by subtracting the same quantity evaluated in BTZ space: $iG^>_{\rm th}(2|1) = \langle\hat{\phi}(v_4,x_4,z_4)\hat{\phi}(v_3,x_3,z_3)\rangle|_{\rm BTZ}$. Applying (3) to BTZ background with fictitious hypersurfaces $v_2 = v_1 = 0$, we obtain

$$G^>_{\rm th}(4|3) = \int dz_1 dx_1 dz_2 dx_2 G^>_{\rm th}(2|1) \times \overleftrightarrow{D}^{v1}\overleftrightarrow{D}^{v2} G^R_{\rm th}(3|1)G^R_{\rm th}(4|2). \tag{5}$$

Subtracting (5) from (3) and noting that D^v is the same for AdS and BTZ spaces, we obtain

$$\Delta G^>(4|3) = \int dz_1 dx_1 dz_2 dx_2 \Delta G^>(2|1) \times \overleftrightarrow{D}^{v1}\overleftrightarrow{D}^{v2} G^R_{\rm th}(3|1)G^R_{\rm th}(4|2), \tag{6}$$

with $\Delta G^>(4|3) = G^>(4|3) - G^>_{\rm th}(4|3)$ being the difference between bulk correlators in the Vaidya background and BTZ background and $\Delta G^>(2|1) = G_0^>(2|1) - G^>_{\rm th}(2|1)$ being the initial value for $\Delta G^>(4|3)$. Below we show that $\Delta G^>(2|1)$ is free of singularity. It is useful to note that AdS_3 and BTZ metrics are related by coordinate transformation.

$$ds^2_{\rm AdS} = \frac{1}{z^2}\left(-(1-z^2)dt^2 + \frac{dz^2}{1-z^2} + dx^2\right),$$
$$ds^2_{\rm BTZ} = \frac{1}{\bar{z}^2}(-d\bar{t}^2 + d\bar{z}^2 + d\bar{x}^2). \tag{7}$$

The explicit coordinate transformation is given by

$$\begin{aligned}\bar{x} &= \sqrt{1-z^2}e^x \cosh t,\\ \bar{t} &= \sqrt{1-z^2}e^x \sinh t,\\ \bar{z} &= ze^x.\end{aligned} \tag{8}$$

The bulk-bulk correlator in Euclidean AdS is known [28],

$$G_E(2|1) = \frac{2^{-\Delta}C_\Delta}{2\Delta-d}\xi^\Delta F\left(\frac{\Delta}{2},\frac{\Delta+1}{2};\Delta-\frac{d}{2}+1,\xi^2\right). \tag{9}$$

For our case of interest $\Delta = d = 2$, G_E is reduced to

$$G_E(2|1) = \frac{1}{4\pi}\left(\frac{1}{\sqrt{1-\xi^2}}-1\right). \tag{10}$$

Using analytic continuation and the coordinate transformation, we obtain the following:

$$\begin{aligned}iG_0^>(2|1) &= G_E\left(\xi = \frac{2z_2z_1}{z_2^2+z_1^2-(v_2-v_1+z_2-z_1-i\epsilon)^2+(x_{21})^2}\right),\\ iG_{\rm th}^>(2|1) &= G_E\left(\xi = \frac{z_2z_1}{\cosh(x_{21})-\sqrt{1-z_2^2}\sqrt{1-z_1^2}\cosh(v_2-v_1+y_2-y_1-i\epsilon)}\right),\end{aligned} \tag{11}$$

with $y_i = -\frac{1}{2}\ln\frac{1-z_i}{1+z_i}$, $i = 1, 2$. We have also used the shorthand notation $x_{ij} = x_i - x_j$. From (11), we find that both $G_0^>$ and $G_{\rm th}^>$ have singularities as $v_2, v_1 \to 0$ and $x_{21} \to 0$. In this case $\xi \to 1$ and $i\epsilon$-prescription become relevant. The singularities arise when the two points pinch $ds^2 \to 0$ [according to (1)] thus owing to short distance physics. Indeed the singularity disappears in the difference $\Delta G^>(2|1)$, which allows us to drop the $i\epsilon$-prescription:

$$i\Delta G^>(2|1) = G_E\left(\xi = \frac{2z_2z_1}{2z_2z_1+(x_{21})^2}\right) - G_E\left(\xi = \frac{z_2z_1}{\cosh(x_{21})-1+z_2z_1}\right). \tag{12}$$

By taking a different limit $z_1 \to 0$, $z_2 \to 0$ of (11), we can also obtain the Wightman correlators in the vacuum and thermal state of $1+1$D CFT:

$$\begin{aligned}iG_0^>(2|1) &= \frac{2}{\pi}\frac{1}{(-(v_2-v_1-i\epsilon)+x_{21})^2},\\ iG_{\rm th}^>(2|1) &= \frac{1}{2\pi}\frac{1}{(-\cosh(v_2-v_1-i\epsilon)+\cosh x_{21})^2}.\end{aligned} \tag{13}$$

Now we turn to the propagators $G_{\rm th}^R(3|1)$ and $G_{\rm th}^R(4|2)$. To be specific, we discuss $G_{\rm th}^R(3|1)$ as an example. It is given by

$$\begin{aligned}iG_{\rm th}^R(3|1) &= i(G_{\rm th}^>(3|1)-G_{\rm th}^<(3|1))\theta(t_3-t_1)\\ &= \left[G_E\left(\xi = \frac{z_3z_1}{\cosh(x_{31})-\sqrt{1-z_3^2}\sqrt{1-z_1^2}\cosh(v_3-v_1+y_3-y_1-i\epsilon)^2}\right)\right.\\ &\quad \left. - G_E\left(\xi = \frac{z_3z_1}{\cosh(x_{31})-\sqrt{1-z_3^2}\sqrt{1-z_1^2}\cosh(v_3-v_1+y_3-y_1+i\epsilon)^2}\right)\right]\theta(t_3-t_1).\end{aligned} \tag{14}$$

In the limit $z_3 \to 0$ needed in the calculation of the boundary correlator, the propagator simplifies:

$$\begin{aligned}G_{\rm th}^R(3|1) = -\frac{i}{8\pi}z_3^2\left[\frac{z_1^2}{(\cosh(x_{31})-\sqrt{1-z_1^2}\cosh(v_3-y_1-i\epsilon))^2}\right.\\ \left. - \frac{z_1^2}{(\cosh(x_{31})-\sqrt{1-z_1^2}\cosh(v_3-y_1+i\epsilon))^2}\right]\theta(t_3-t_1),\end{aligned} \tag{15}$$

where we have used $v_1 = 0$. Note that the propagator is only nonvanishing on the light cone:

$$\cosh(x_{31}) = \sqrt{1 - z_1^2}\cosh(v_3 - y_1). \tag{16}$$

Since $\cosh(x_{31}) \geq 1$, it follows that $v_3 \geq 2y_1$. It is convenient to write (15) as derivative of a delta function:

$$G^R_{\rm th}(3|1) = -\frac{1}{4}z_3^2 z_1^2 \delta'(\cosh(x_{31}) - \cosh(v_3) + \sinh(v_3)z_1). \tag{17}$$

Now we can use $G^R_{\rm th}(3|1)$ to propagate point 1 to point 3. We use the delta function to eliminate the integration of z_1.[1] The following trick is used:

$$\begin{aligned}
&\int dz_1 \Delta G^>(2|1) \overset{\leftrightarrow}{D}{}^{v1} G^R_{\rm th}(3|1) \\
&= \int dz_1 \Delta G^>(2|1)\left(-\frac{1}{z_1}\overset{\leftrightarrow}{\partial}_{z1}\right) G^R_{\rm th}(3|1) \\
&= \int dz_1 \frac{\Delta G^>(2|1)}{\sqrt{z_1}}(-\overset{\leftrightarrow}{\partial}_{z1})\frac{G^R_{\rm th}(3|1)}{\sqrt{z_1}} \\
&= \int dz_1 2\partial_{z1}\left(\frac{\Delta G^>(2|1)}{\sqrt{z_1}}\right)\frac{G^R_{\rm th}(3|1)}{\sqrt{z_1}}.
\end{aligned} \tag{18}$$

We have redistributed the factor $\frac{1}{z_1}$ into $\Delta G^>(2|1)$ and $G^R_{\rm th}(3|1)$. This is justified because the terms from derivatives on $\frac{1}{\sqrt{z_1}}$ cancel pairwise. We have also used partial integration in the last step because $G^R_{\rm th}(3|1)$ only has finite support on z_1. Now we are ready to put everything together to obtain

$$\begin{aligned}
\Delta G^>(4|3) = &\int dz_1 dx_1 dz_2 dx_2 \partial_{z1}\partial_{z2} \\
&\times \left(\frac{\Delta G^>(2|1)}{\sqrt{z_2 z_1}}\right)(z_2 z_1)^{3/2}\delta'(\cosh(x_{31}) - \Gamma_1)\delta' \\
&\times (\cosh(x_{42}) - \Gamma_2),
\end{aligned} \tag{19}$$

where

$$\begin{aligned}
\Gamma_1 &= \cosh(v_3) - \sinh(v_3)z_1, \\
\Gamma_2 &= \cosh(v_4) - \sinh(v_4)z_2.
\end{aligned} \tag{20}$$

Careful elimination of the delta functions in (19) leads to

$$\begin{aligned}
&\Delta\langle O(v_4, x_4)O(v_3, x_3)\rangle \\
&= \int dx_{31}dx_{42}\frac{\partial z_1}{\partial \Gamma_1}\frac{\partial z_2}{\partial \Gamma_2}\partial_{z1}\partial_{z2} \\
&\quad\times\left[\frac{\partial z_1}{\partial \Gamma_1}\frac{\partial z_2}{\partial \Gamma_2}\partial_{z1}\partial_{z2}\left(\frac{i\Delta G^>(2|1)}{\sqrt{z_2 z_1}}\right)(z_2 z_1)^{3/2}\right] \\
&= \frac{1}{\sinh^2 v_3 \sinh^2 v_4}\int dx_{31}dx_{42}\partial_{z1}\partial_{z2} \\
&\quad\times\left[\partial_{z1}\partial_{z2}\left(\frac{i\Delta G^>(2|1)}{\sqrt{z_2 z_1}}\right)(z_2 z_1)^{3/2}\right],
\end{aligned} \tag{21}$$

with $z_1 = \frac{\cosh(v_3)-\cosh(x_{31})}{\sinh(v_3)}$ and $z_2 = \frac{\cosh(v_4)-\cosh(x_{42})}{\sinh(v_4)}$. The integrations of x_{31} and x_{42} are bounded by $|x_{31}| \leq v_3$ and $|x_{42}| \leq v_4$ respectively. By construction, $\Delta\langle O(v_4, x_{43})O(v_3, 0)\rangle$ is the difference of correlation in the thermalizing state minus the counterpart in the thermal state:

$$\begin{aligned}
&\Delta\langle O(v_4, x_4)O(v_3, x_3)\rangle \\
&\quad = \langle O(v_4, x_{43})O(v_3, 0)\rangle - \langle O(v_4, x_{43})O(v_3, 0)\rangle_{\rm th}.
\end{aligned} \tag{22}$$

We evaluate (21) in different kinematic regimes and show the results in the next section.

III. RESULTS IN COORDINATE SPACE

We are interested in two classes of correlators: (i.) equal-time correlator $\Delta\langle O(v, x)O(v, 0)\rangle$ and (ii.) equal-space correlator $\Delta\langle O(v_4, 0)O(v_3, 0)\rangle$. The first class measures evolution of spatial correlation, and the second class measures the evolution of temporal correlation. We evaluate them separately.

A. Equal-time correlator

We start from the definition (22). For the equal-time correlator, only the first term evolves with time v. The second term is stationary. At initial time of thermalization $v = 0$, we expect the first term to reduce to the vacuum correlator. According to (13), we obtain

$$\Delta\langle O(v, x)O(v, 0)\rangle \xrightarrow{v\to 0} \frac{2}{\pi}\frac{1}{x^4} - \frac{1}{2\pi}\frac{1}{(-1 + \cosh x)^2}. \tag{23}$$

We see that the first term is a power law decay in separation, which indicates long range correlation in the vacuum of CFT. The second term features an exponential decay, which characterizes Debye screening, with the screening length set by $1/T \sim 1$ in our unit. From now on, we specialize to two limiting cases: $x \gg 1$ and $x \ll 1$. The two cases correspond to the spatial separation much larger/smaller than the spatial screening length.

When $x \gg 1$, we can ignore the exponential decaying term. $\Delta\langle O(v, x)O(v, 0)\rangle$ simply measures decay of the vacuum correlator. For this reason, we parametrize the correlator as $\Delta\langle O(v, x)O(v, 0)\rangle = \frac{1}{x^4}\mathcal{F}(v)$. The decaying

[1] We could eliminate the integration of x_1 instead, but then the integration of z_1 sees a divergence as $y_1 \to v_3/2$. This is not a true divergence but requires more careful treatment of the delta function.

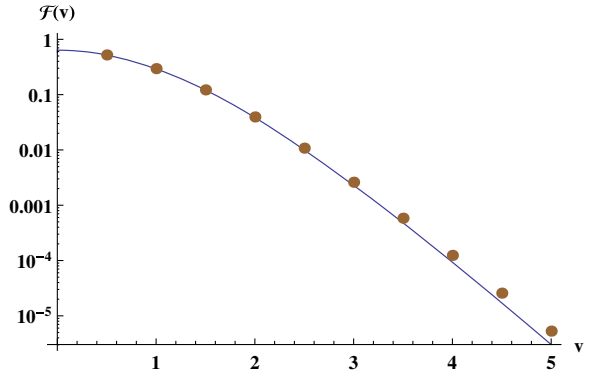

FIG. 1. $\mathcal{F}(v) = x^4\Delta\langle O(v,x)O(v,0)\rangle$ as a function of v for $x = 15$. The analytic fitting function is given by $\frac{18}{\pi}(\frac{v\coth v-1}{\sinh^2 v})^2$. It fits very well in a wide range of v.

function $\mathcal{F}(v)$ can be obtained from numerical integration of (21). Figure 1 shows numerical results of $\mathcal{F}(v)$. We also include analytic approximation of $\mathcal{F}(v)$. The specific form of the analytic expression will be obtained later. Next we consider $x \ll 1$. In this case, the leading $\frac{1}{x^4}$ behavior in vacuum and thermal correlators cancels out. (23) reduces to

$$\Delta\langle O(v,x)O(v,0)\rangle \xrightarrow{v\to 0} \frac{1}{3\pi}\frac{1}{x^2}. \tag{24}$$

We further restrict ourselves to the regime $v \ll 1$. In this regime, we expect the following scaling: $\Delta\langle O(v,x)O(v,0)\rangle = \frac{1}{x^2}\mathcal{G}(\frac{v}{x})$. In Fig. 2, we confirm the scaling behavior by showing numerical results of $\mathcal{G}(\frac{v}{x})$ obtained when different x agree with each other. However, we do not have an analytic expression for the scaling function $\mathcal{G}(\frac{v}{x})$.

B. Analytic results for the spacelike correlator

It is a good point to present analytic results for spacelike correlator $\langle O(v_4,x_{43})O(v_3,0)\rangle$, which include the equal-time correlator discussed in the previous subsection. One

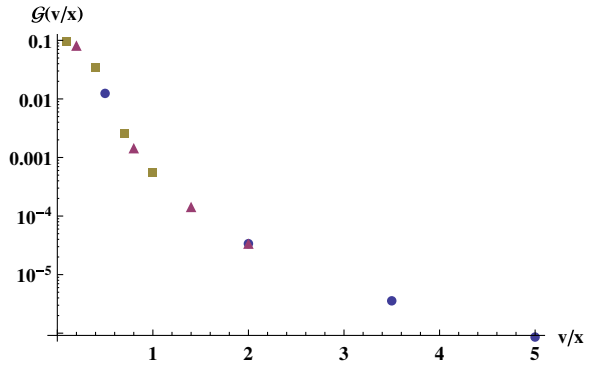

FIG. 2. $\mathcal{G}(v/x) = x^2\Delta\langle O(v,x)O(v,0)\rangle$ as a function of v/x for $x = 1/50$(blue point), $x = 1/20$(purple triangle) and $x = 1/10$(brown square). The tail is numerically consistent with a power law $\mathcal{G}(\frac{v}{x}) \sim (\frac{x}{v})^4$.

limit allowing for analytic treatment is $x_{43} \gg 1$, $x_{43} \gg v_3, v_4$. In this case, $x_{21} = x_{43} - x_{42} + x_{31} \simeq x_{43}$ because $|x_{31}| \le v_3$, $|x_{42}| \le v_4$ and $|x_{43}| \gg v_3$, v_4. Since $x_{21} \simeq x_{43} > 0$, we have $\xi < 1$; thus regularization is not needed. We can calculate $\langle O(v_4,x_{43})O(v_3,0)\rangle$ directly. This is possible as long as $x_{43} > v_4 + v_3$, which can be viewed as a generalized spacelike condition for correlator $\langle O(v_4,x_{43})O(v_3,0)\rangle$. To proceed, we note $x_{43} \gg 1 > z_1 z_2$; therefore we can approximate the invariant distance in AdS

$$\xi_{\rm AdS} = \frac{2z_2z_1}{2z_2z_2 + x_{21}^2} \simeq \frac{2z_2z_1}{x_{43}^2} \ll 1. \tag{25}$$

Note that $G_E(\xi) \sim \xi^2$ as $\xi \to 0$. As a result, $\Delta G^>(2|1)$ simplifies significantly:

$$iG^>(2|1) \simeq \frac{\xi_{\rm AdS}^2}{8\pi} \simeq \frac{1}{8\pi}\left(\frac{2z_2z_1}{x_{43}^2}\right)^2. \tag{26}$$

With (26), we can evaluate (21) analytically to obtain

$$\langle O(v_4,x_4)O(v_3,x_3)\rangle \simeq \frac{18}{\pi x_{43}^4}\frac{v_3\coth(v_3)-1}{\sinh^2(v_3)}\frac{v_4\coth(v_4)-1}{\sinh^2(v_4)}. \tag{27}$$

Note that (27) is valid for arbitrary v_3, v_4 as long as $x_{43} \gg v_3$, v_4. (27) gives the fitting function in Fig. 1 upon setting $v_3 = v_4 = v$. It gives for v_3, $v_4 \ll 1$

$$\langle O(v_4,x_4)O(v_3,x_3)\rangle \simeq \frac{2}{\pi x_{43}^4}, \tag{28}$$

which reproduces Eq. (5.7) of [1]. On the other hand, for v_3, $v_4 \gg 1$

$$\langle O(v_4,x_4)O(v_3,x_3)\rangle \simeq \frac{18}{\pi x_{43}^4} v_3 v_4 e^{-2v_3-2v_4}, \tag{29}$$

while the geodesic approximation in [1] gives

$$\langle O(v_4,x_4)O(v_3,x_3)\rangle \sim \frac{1}{x_{43}^4} e^{-2v_3-2v_4}. \tag{30}$$

We note that the geodesic approximation misses the enhancement factor v_3v_4 in the spacelike correlator. It is not difficult to understand the reason from the gravity point of view: since geodesic approximation only knows about the bulk geometry lying between boundary insertion times v_3 and v_4, the enhancement factor results from the history of the bulk geometry (from the time of energy injection $v = 0$ to the times of measurement at v_3 and v_4).

It is informative to compare our results with general results obtained by CC [15]. In the latter case, the correlator $\langle O(v_4,x)O(v_3,0)\rangle$ in a thermalizing state is given by

$$\langle O(v_4,x_{43})O(v_3,0)\rangle \sim \begin{cases} e^{-2\pi(v_3+v_4)/2\tau_0} & x_{43} > v_3+v_4 \\ e^{-2\pi x_{43}/2\tau_0} & |v_4-v_3| < x_{43} < v_3+v_4 \\ e^{-2\pi|v_4-v_3|/2\tau_0} & x_{43} < |v_4-v_3|. \end{cases} \quad (31)$$

τ_0 is proportional to inverse temperature adapted to our model. Comparing (31) in the long time (thermal) limit with (13), we identify $2\tau_0=\pi$. However, (31) does not contain the power law factor $1/x_{43}^4$ present in (29). As already pointed out in [1], it is because the initial state in the formulation of CC has finite correlation length, while the power law is reminiscent of long range correlation present in the initial state modeled by the Vaidya background. We argue now that the time factor v_3v_4 missed in geodesic approximation is also due to the long range correlation in the initial state: as $\langle \Delta O(v_4,x_4)O(v_3,x_3)\rangle$ receives contribution from regions in the backward light cone, factors of v_3 and v_4 come from the distance of the correlated regions that propagate initial state correlation to point x_3 and x_4 respectively.

We note that in the case of CC (31), a spacelike correlator $\langle O(v_4,x_{43})O(v_3,0)\rangle$ changes from exponential decaying form $e^{-2(v_3+v_4)}$ to thermal form $e^{-2x_{43}}$ when v_3+v_4 exceeds x_{43}, up to correction of order inverse temperature. If we define thermalization time to be the largest possible value of v_3 or v_4 across which the correlator $\langle O(v_4,x_{43})O(v_3,0)\rangle$ appears thermal, (31) implies that points separated by distance x_{43} take a time $x_{43}+O(1)$ to thermalize.[2] When the initial state has long range correlation, the spacelike correlator $\langle \Delta O(v_4,x_{43})O(v_3,0)\rangle$ is modified by power law factor v_3v_4/x_{43}^4. This seems to imply that the thermalization time could be modified to $x_{43}+O(\ln x_{43})$. We show below that it is not the case.

It is desirable to find analytic results for the correlator near the light cone: $v_3+v_4\simeq x_{43}$. It turns out to be possible in the following regime: $x_{43}\gg 1$ and $x_{43}-v_4\equiv\delta\sim O(1)\gg v_3$. We consider $\delta>0$, which satisfies generalized spacelike condition $x_{43}-v_4-v_3>0$; thus regularization is not needed. We evaluate $\langle O(v_4,x_{43})O(v_3,0)\rangle$ directly and compare to the thermal correlator $\langle O(0,x_{43})O(0,0)\rangle_{\rm th}$. In the regime we work in, $x_{21}=x_{43}-x_{42}+x_{31}>x_{43}-v_4-v_3\simeq\delta$. Furthermore $z_1<\frac{\cosh v_3-1}{\sinh v_3}=\tanh\frac{v_3}{2}\ll\delta$ and $z_2<1$; thus $x_{21}\gg z_1z_2$. Combining the above, we can approximate

$$\xi_{\rm AdS}\simeq\frac{2z_2z_1}{x_{43}-x_{42}}. \quad (32)$$

The integration of x_{31} and x_{42} factorizes. The integration of x_{31} and x_{42} can be done separately as follows:

$$\int_{-v_3}^{v_3}dx_{31}\frac{z_1}{\sinh^2 v_3}=\frac{2(v_3\coth v_3-1)}{\sinh^2 v_3},$$
$$\int_{-v_4}^{v_4}dx_{42}\frac{z_2}{\sinh^2 v_4}\frac{1}{(x_{43}-x_{42})^4}$$
$$=\frac{1}{\sinh^3 v_4}\left[\frac{\cosh v_4-\cosh x_{42}}{3(x_{43}-x_{42})^3}+\frac{\sinh x_{42}}{6(x_{43}-x_{42})^2}\right.$$
$$-\frac{\cosh x_{42}}{6(x_{43}-x_{42})}-\frac{1}{12}(e^{x_{43}}Ei(x_{42}-x_{43})$$
$$\left.-e^{-x_{43}}Ei(x_{43}-x_{42}))\right]\Big|_{x_{42}=-v_4}^{v_4}. \quad (33)$$

Working in the limit $v_4\gg 1$, $v_3\ll 1$ of (33), we find the x_{31} integral approaches a constant, and the x_{42} integral asymptotes to

$$\frac{e^{-2v_4}}{12}\left(\frac{1}{\delta^2}-\frac{1}{\delta}-e^{\delta}Ei(-\delta)\right). \quad (34)$$

The correlator $\langle O(v_4,x_{43})O(v_3,0)\rangle$ given by the product of two integrals in (33) (up to overall numerical factor) does not have enhancement factor v_4 close to the light cone. Comparing (34) with thermal correlator $e^{-2x_{43}}$, we conclude that the thermalization time in this case is given by $v_4+O(1)\simeq x_{43}+O(1)$, thus free from $\ln x_{43}$ correction. For completeness, we also plot the function in the bracket of (34) in Fig. 3, which is a monotonously decreasing function of δ.

We have also performed numerical studies of equal-time correlator $\langle O(v,x)O(v,0)\rangle$ for large v and x near the generalized light cone $x=2v$. Defining the point at which the equal-time correlator drops to twice the thermal correlator as the thermalization time, we find the thermalization time is still given by $v\simeq x+O(1)$, free from correction of order $\ln x$.

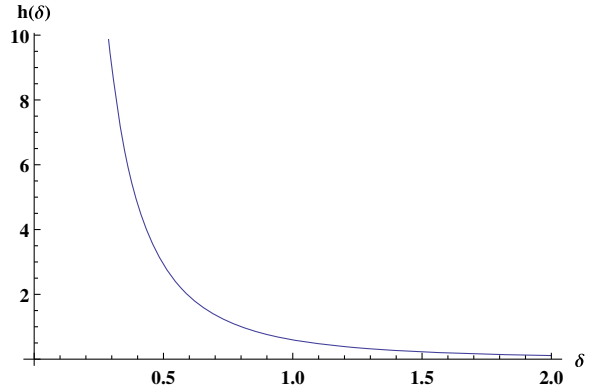

FIG. 3. $h(\delta)\equiv\frac{1}{\delta^2}-\frac{1}{\delta}-e^{\delta}Ei(-\delta)$ as a function of δ. It is a monotonously decreasing function of δ. As $\delta\to 0$, the two insertion points $(v_4,x_{43}=v_4+\delta)$ and $(v_3,0)(v_3\ll 1)$ approach the light cone. The dropping of $h(\delta)$ corresponds to the thermalization of the correlator, which occurs on a time scale of $O(1)$.

[2]This is realized when $v_4\to x_{43}$ and $v_3\to 0$ for example.

C. Equal-space correlator

Now we look at equal-space correlator $\Delta\langle O(v_4,0)O(v_3,0)\rangle$ with $v_4 \equiv v+\delta v$ and $v_3 \equiv v$. Parallel to the equal-time case, we study the regimes $\delta v \ll 1$ and $\delta v \gg 1$. Similar to the equal-time correlator, we might expect equal-space correlator $\Delta\langle O(v+\delta v,0)O(v,0)\rangle$ to reduce to the difference between the vacuum and thermal correlator as $v \to 0$, which is

$$\Delta\langle O(v+\delta v,0)O(v,0)\rangle \xrightarrow{v\to 0} \frac{2}{\pi}\frac{1}{\delta v^4} - \frac{1}{2\pi}\frac{1}{(-1+\cosh \delta v)^2}. \tag{35}$$

In the regime $\delta v \ll 1$, that is, when the temporal separation is much less than the screening length, (35) reduces to $\frac{1}{3\pi}\frac{1}{\delta v^2}$. This motivates the following scaling behavior for $\Delta\langle O(v+\delta v,0)O(v,0)\rangle = \frac{1}{\delta v^2}\mathcal{H}(\frac{v}{\delta v})$ when $\delta v \ll 1$, $v \ll 1$. Indeed, we can confirm the scaling behavior from numerical results. Figure 4 shows the scaling function $\mathcal{H}(\frac{v}{\delta v})$ for different δv. However, the expectation (35) turns out to be incorrect. The expectation would predict that $\mathcal{H}(\frac{v}{\delta v})$ approaches the constant $\frac{1}{3\pi}$, while the numerical results blow up as $\frac{v}{\delta v} \to 0$. Interestingly, if we consider the limit $\delta v \to 0$, the correlator $\Delta\langle O(v+\delta v,0)O(v,0)\rangle$ always gives a finite value. This shows a noncommutativity between the limit $v \to 0$ and $\delta v \to 0$.

Now we study the regime $\delta v \gg 1$. We would like to find the thermalization time for temporal interval $\delta v \gg 1$. For the equal-space correlator, CC results (31) imply a thermalization time of order inverse temperature, independent of δv. We define thermalization time to be v at which $\Delta\langle O(v+\delta v,0)O(v,0)\rangle$ drops to the thermal correlator $\langle O(\delta v,0)O(0,0)\rangle_{\text{th}}$. We perform numerical studies and find $\Delta\langle O(v+\delta v,0)O(v,0)\rangle \sim e^{-2\delta v}$ for $\delta v \gg 1$ and $v = O(1)$. On the other hand, $\langle O(\delta v,0)O(0,0)\rangle_{\text{th}} \sim e^{-2\delta v}$. Figure 5 includes a plot of $r(v) \equiv \Delta\langle O(v+\delta v,0)O(v,0)\rangle / \langle O(\delta v,0)O(0,0)\rangle_{\text{th}}$.

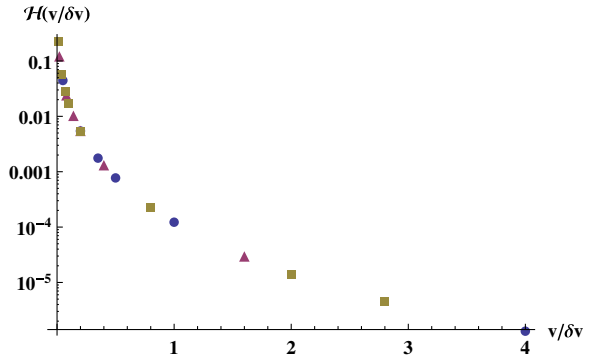

FIG. 4. $\mathcal{H}(v/\delta v) = \delta v^2 \Delta\langle O(v+\delta v,0)O(v,0)\rangle$ as a function of $v/\delta v$ for $\delta v = 1/50$ (blue point), $\delta v = 1/20$ (purple triangle) and $\delta v = 1/10$ (brown square) falls onto the same scaling curve.

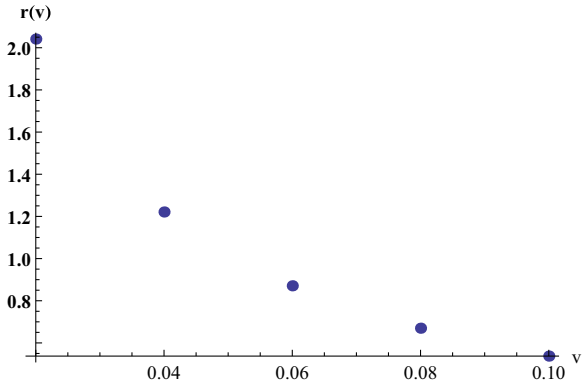

FIG. 5. $r(v) = \Delta\langle O(v+\delta v,0)O(v,0)\rangle / \langle O(\delta v,0)O(0,0)\rangle_{\text{th}}$ as a function of v for $\delta v = 10$. It is a monotonously decreasing function of order one, indicating a thermalization time of order inverse temperature for large temporal interval.

Summarizing this section, we have found analytic expressions of the equal-time correlator and spacelike correlator near the light cone. While the expressions deviate from CC and holographic results obtained with geodesic approximation, the thermalization time is not significantly modified due to the presence of long range correlation in the initial state: a thermalization time $x_{43} + O(1/T)$ for spacelike correlator $\Delta\langle O(v_4,x_{43})O(v_3,0)\rangle$ and a thermalization time $O(1/T)$ for equal-space correlator $\Delta\langle O(v+\delta v)O(v,0)\rangle$.

IV. RESULTS FOR THE SPATIALLY INTEGRATED CORRELATOR

In this section, we work in (spatial) momentum space, but still use temporal coordinates. In particular, we focus on the spatially integrated correlator, i.e. the mode with $k = 0$. Fourier transform of (21) gives us

$$\begin{aligned}\int dx_{43}\Delta\langle O(v_4,x_4)O(v_3,x_3)\rangle &= \int dx_{31}dx_{42}\frac{\partial z_1}{\partial \Gamma_1}\frac{\partial z_2}{\partial \Gamma_2}\partial_{z1}\partial_{z2} \\ &\times \left[\frac{\partial z_1}{\partial \Gamma_1}\frac{\partial z_2}{\partial \Gamma_2}\partial_{z1}\partial_{z2}\left(\int dx_{21}\frac{i\Delta G^{>}(2|1)}{\sqrt{z_2 z_1}}\right)(z_2 z_1)^{3/2}\right].\end{aligned} \tag{36}$$

The spatially integrated initial value is given by

$$\int dx_{21} i\Delta G^{>}(2|1) = \int dx_{21} i(G_0^{>}(2|1) - G_{\text{th}}^{>}(2|1)). \tag{37}$$

The integration of $G_0^{>}(2|1)$ is easily done, with the following result,

$$\int dx_{21} i G_0^{>}(2|1) = \frac{\sqrt{b}}{2\pi} Q_{1/2}\left(1-\frac{\epsilon}{b}\right), \tag{38}$$

where $b = z_2 z_1$ and $\epsilon = (v_2 - v_1)(z_2 - z_1)$. The integration of $iG^{>}_{\rm th}(2|1)$ requires some effort,

$$\frac{1}{4\pi}\int_{-\infty}^{+\infty} dx_{21}\left(\frac{1}{\sqrt{1-\xi^2_{\rm BTZ}}}-1\right) = \frac{1}{2\pi}\int_1^{\infty}\frac{ds}{\sqrt{s^2-1}}\left(\frac{s-a}{\sqrt{(s-a+b)(s-a-b)}}-1\right), \tag{39}$$

where $a = \sqrt{1-z_2^2}\sqrt{1-z_1^2}(\cosh(v_2 - v_1 + y_2 - y_1))$. In the limit $v_2,\ v_1 \to 0$ relevant for our initial condition, $a = 1 - b + \epsilon$. In calculating the integral in (39), we note that separate integrations of two terms in the bracket both diverge, but the divergences cancel out in the their difference yielding a finite result. We calculate (39) from the regulated integral

$$\int_1^{\Lambda}\frac{ds}{\sqrt{s^2-1}}\left(\frac{s-a+b}{s-a-b}\right)^{1/2} + \int_1^{\Lambda}\frac{ds}{\sqrt{s^2-1}}\left(\frac{s-a-b}{s-a+b}\right)^{1/2} - 2\int_1^{\Lambda}\frac{ds}{\sqrt{s^2-1}}. \tag{40}$$

The limit $\Lambda \to \infty$, $\epsilon \to 0$ of the above integral can be obtained analytically. We only show the final result and collect technical details in the Appendix.

$$\int dx_{21} iG^{>}_{\rm th}(2|1) = \frac{(-4\ln(1+\sqrt{b}) - \sqrt{b}(2\ln(1+\frac{1}{\sqrt{b}}) + \ln\frac{\epsilon}{32}))}{4\pi}. \tag{41}$$

We see that although (38) and (41) contain separate logarithmic divergences in ϵ (light cone singularities), the divergences cancel out in their difference:

$$\int dx_{21} i(G^{>}_0(2|1) - G^{>}_{\rm th}(2|1)) = \frac{(-2\sqrt{b} + (2+\sqrt{b})\ln(1+\sqrt{b}))}{2\pi}. \tag{42}$$

Plugging (42) into (36), we obtain the following simple representation,

$$\int dx_{43}\Delta\langle O(v_4,x_4)O(v_3,x_3)\rangle = \frac{3}{16\pi\sinh^2(v_3)\sinh^2(v_4)}\int dx_{31}dx_{42}\frac{\sqrt{z_2 z_1}}{(1+\sqrt{z_2 z_1})^4}, \tag{43}$$

with $z_1 = \frac{\cosh(v_3)-\cosh(x_{31})}{\sinh(v_3)}$ and $z_2 = \frac{\cosh(v_4)-\cosh(x_{42})}{\sinh(v_4)}$. We consider the regime $v_3 \ll 1$ and v_4 arbitrary. This regime allows us to do the integral analytically. Note that $z_1 \le \frac{\cosh(v_3)-1}{\sinh(v_3)} \le v_3 \ll 1$ and $z_2 \le 1$. We can then drop $\sqrt{z_2 z_1}$ in the denominator and the integral can be expressed in terms of elliptic integrals

$$\int dx_{43}\Delta\langle O(v_4,x_4)O(v_3,x_3)\rangle \simeq \frac{3\sqrt{2}}{16\sqrt{v_3}}\frac{\sqrt{\coth(v_4/2)}}{\sinh^2(v_4)} \times (K(\tanh(v_4/2)) - E(\tanh(v_4/2))). \tag{44}$$

We consider the early time and late time regime of (44). At early time $v_4 \ll 1$, we obtain

$$\int dx_{43}\Delta\langle O(v_4,x_4)O(v_3,x_3)\rangle \simeq \frac{3\pi}{128\sqrt{v_3 v_4}}. \tag{45}$$

The dependence $\frac{1}{\sqrt{v_3 v_4}}$ can be understood in the following way: We claim that the spatial integration receives dominant contribution from the domain with $x_{43} \ll 1$, i.e. short distance. This is most easily seen in equal-time correlator $\Delta\langle O(v,x)O(v,0)\rangle$. For $v,\ x \ll 1$, the equal-time correlator is given by

$$\Delta\langle O(v,x)O(v,0)\rangle = \frac{1}{x^2}\mathcal{G}\left(\frac{v}{x}\right). \tag{46}$$

Integrating the above over x, we obtain $\sim\frac{1}{v}$. Numerically integrating the scaling function $\mathcal{G}(\frac{v}{x})$, we can confirm the numerical factor in (45). Therefore, the spatially integrated equal-time correlator in the far from equilibrium regime receives dominant contribution from short distance physics. This is in contrast to the equilibrium intuition that small momentum is equivalent to long distance physics. With more sophisticated analysis, we could show that the conclusion remains true for the more generic correlator $\Delta\langle O(v_4,x_{43})O(v_3,0)\rangle$. At late time $v_4 \gg 1$, we obtain

$$\int dx_{43}\Delta\langle O(v_4,x_4)O(v_3,x_3) \simeq \frac{3\sqrt{2}}{32\sqrt{v_3}} v_4 e^{-2v_4}. \tag{47}$$

A. Out-of-equilibrium emission spectrum

As an application, we calculate a physical observable: emission spectrum of particles weakly coupled to operator O. We can draw an analogy with dilepton emission: we can regard O as current, and radiated particles as dilepton. The coupling constant g_O between radiated particle and O is small like the electromagnetic coupling e. With an abuse of terminology, we refer to the radiated particle as dilepton and the field created by O as photon. In the absence of translational invariance in time, we use the following operational definition for the local emission rate of dilepton: as the dilepton is being radiated continuously in the

thermalization process, we define the differential yield at time v as the emission rate. We formulate the differential rate as follows: the transition amplitude from an initial state $|i\rangle$ to a final state $|f\rangle$ with photon is given by

$$S_{fi} = g_O \int d^2X e^{iQX} \langle f|O(X)|i\rangle. \tag{48}$$

The total yield of dilepton is given by

$$\begin{aligned}\sum_f |S_{fi}|^2 &= g_O^2 \int d^2X d^2Y e^{iQ(X-Y)} \\ &\quad \times \sum_f \langle i|O(Y)|f\rangle\langle f|O(X)|i\rangle \\ &= g_O^2 \int d^2X d^2Y e^{iQ(X-Y)} \langle i|O(Y)O(X)|i\rangle. \end{aligned} \tag{49}$$

We count the yield through time v; thus the integration of X^0 and Y^0 is taken from $-\infty$ to v. Using translational invariance in spatial direction, we can simplify the total rate as

$$\begin{aligned}\sum_f |S_{fi}|^2 &= g_O^2 \int_{-\infty}^{v} dX^0 \int_{-\infty}^{v} dY^0 V \\ &\quad \times \int d(X^1 - Y^1) e^{iQ(X-Y)} \langle i|O(Y)O(X)|i\rangle, \end{aligned} \tag{50}$$

where V is the one-dimensional volume. We have used spatial translation invariance in (50). Now we identify (50) with spacetime integral of differential emission rate

$$\begin{aligned} V \int_{-\infty}^{v} dt \frac{d\Gamma(t)}{d^2Q} &= g_O^2 \int_{-\infty}^{v} dX^0 \int_{-\infty}^{v} dY^0 V \\ &\quad \times \int d(X^1 - Y^1) e^{iQ(X-Y)} \langle i|O(Y)O(X)|i\rangle. \end{aligned} \tag{51}$$

Canceling the volume factor and taking the derivative with respect to v, we obtain the following representation of differential rate:

$$\begin{aligned} \frac{d\Gamma(\omega, v)}{d^2Q} &= g_O^2 \left[\int_{-\infty}^{v} dX^0 e^{i\omega(X^0 - v)}|_{Y^0 = v} \right. \\ &\quad \left. + \int_{-\infty}^{v} dY^0 e^{i\omega(v - Y^0)}|_{X^0 = v} \right] \\ &\quad \times \int d(X^1 - Y^1) e^{-ik(X^1 - Y^1)} \langle i|O(Y)O(X)|i\rangle. \end{aligned} \tag{52}$$

For $k = 0$, the regularized version of the quantity $\int d(X^1 - Y^1) e^{-ik(X^1 - Y^1)} \langle i|O(Y)O(X)|i\rangle$ has already been calculated in (43). To obtain the full result, we add back the thermal part:

$$\begin{aligned} &\int d(X^1 - Y^1) \langle i|O(Y)O(X)|i\rangle \\ &\quad = \int dx_{43} (\Delta\langle O(v_4, x_{43}) O(v_3, 0)\rangle \\ &\qquad + \langle O(v_4, x_{43}) O(v_3, 0)\rangle_{\text{th}}). \end{aligned} \tag{53}$$

The thermal part is given by

$$\begin{aligned} &\int dx_{43} \langle O(v_4, x_{43}) O(v_3, 0)\rangle_{\text{th}} \\ &\quad = \int dx_{43} \frac{1}{2\pi} \frac{1}{(-\cosh(v_4 - v_3 - i\epsilon) + \cosh x_{43})^2} \\ &\quad = \frac{1}{2\pi} \frac{(v_4 - v_3)\coth(v_4 - v_3) - 1}{\sinh^2(v_4 - v_3)}. \end{aligned} \tag{54}$$

From (43) and (54), we can see that $\int d(X^1 - Y^1) \langle i|O(Y)O(X)|i\rangle$ is invariant under exchange of X and Y. It is not difficult to show that the exchange symmetry leads to the spectrum being an even function of ω. Note that (43) is valid only after $v > 0$; therefore the integration of dX^0 and dY^0 starts from $t = 0$ through $t = v$. Before $v = 0$, the state is vacuum state, which does not radiate any dilepton. To compare the emission rate with different frequencies, we normalize the rate by dividing the thermal rate, which is given by the Fourier transform of (54),

$$\frac{d\Gamma(\omega)_{\text{th}}}{d^2Q}(\omega) = g_O^2 \int dt e^{-i\omega t} \frac{1}{2\pi} \frac{t\coth t - 1}{\sinh^2 t}. \tag{55}$$

As a separate reference, we also calculate the emission rate, assuming instantaneous thermalization of the state at $v = 0$. The emission rate in this case is given by

$$\begin{aligned} \frac{d\Gamma_{\text{inst}}(\omega, v)}{d^2Q} &= g_O^2 \left[\int_0^{v} dX^0 e^{i\omega(X^0 - v)}|_{Y^0 = v} \right. \\ &\quad \left. + \int_0^{v} dY^0 e^{i\omega(v - Y^0)}|_{X^0 = v} \right] \\ &\quad \times \int d(X^1 - Y^1) \langle i|O(Y)O(X)|i\rangle_{\text{th}}. \end{aligned} \tag{56}$$

We present our results for $\omega = 1$, $\omega = 2$ and $\omega = 2.5$ in Fig. 6. We see that both $d\Gamma(\omega, v)/d^2Q$ and $d\Gamma_{\text{inst}}(\omega, v)/d^2Q$ approach the thermal rate at large time. The deviation of the former comes from the out-of-equilibrium effect and missing radiation before $v = 0$. The deviation of the latter includes only missing radiation before $v = 0$. We do observe that the rates become negative at early time. We believe this is an artifact of our definition: strictly speaking, we need to know the past and future of radiation in order to define plane wave spectrum, while we only know the history up to our measurement point at v. With the caveat in mind, we do observe interesting hierarchy in frequency: low frequency mode tends to

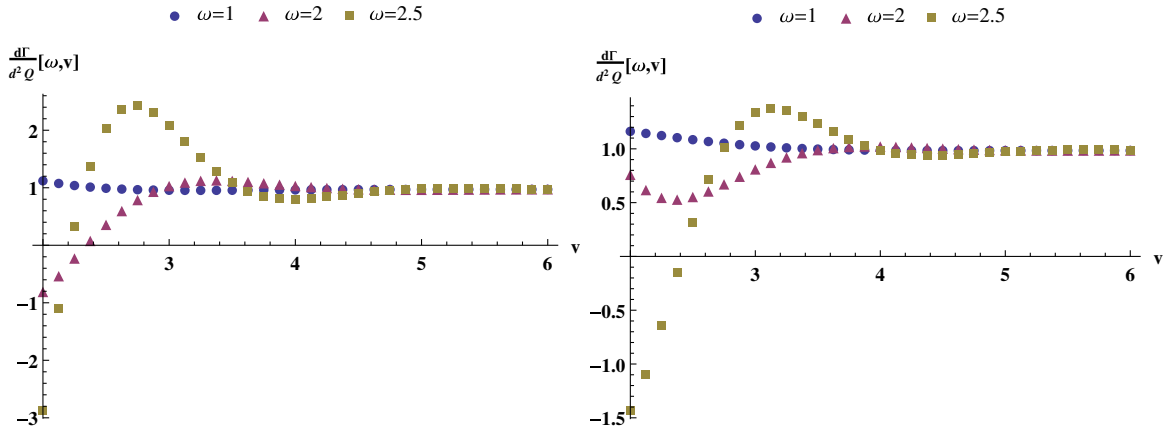

FIG. 6. Emission rates $\frac{d\Gamma}{d^2Q}(\omega, v)$ as a function of v in the thermalizing state (left) and in an instantaneous thermalization scenario (right); see (52)–(56) for corresponding definitions. Both rates are in units of thermal emission rate $\frac{d\Gamma_{\rm th}}{d^2Q}(\omega)$, defined in (55). The symbols represent $\omega = 1$ (blue point), $\omega = 2$ (purple triangle) and $\omega = 2.5$ (brown square). All the rates approach thermal limit at late time. We observe a hierarchy among spectra with different frequencies, with lower frequency mode tending to thermal spectrum faster. The high frequency mode shows more oscillations in relaxing to thermal spectrum. A possible cause for the negative rate at early time is given in the text.

appear thermal faster than high frequency mode. Previous studies have shown that short distance physics tends to thermalize faster than long distance physics. Our results can be viewed as a complementary picture to this, although in a counterintuitive way. We also note that high frequency mode shows more oscillations in relaxing to thermal spectrum.

ACKNOWLEDGMENTS

The author is grateful to E. Shuryak and D. Teaney for insightful discussions, which significantly improved this work. He thanks S. Schlichting, S. Stricker and H.-U. Yee for useful discussions. He also thanks the Institute of Nuclear Theory for hospitality at the workshop "Equilibration Mechanisms in Weakly and Strongly Coupled Quantum Field Theory" in the completion of this work. This work is in part supported by RIKEN Foreign Postdoctoral Researcher Program and Junior Faculty's Fund of Sun Yat-Sen University.

APPENDIX: EVALUATION OF (40)

We reproduce (40) below for easy reference:

$$\int_1^\Lambda \frac{ds}{\sqrt{s^2-1}}\left(\frac{s-a+b}{s-a-b}\right)^{1/2} + \int_1^\Lambda \frac{ds}{\sqrt{s^2-1}}\left(\frac{s-a-b}{s-a+b}\right)^{1/2} - 2\int_1^\Lambda \frac{ds}{\sqrt{s^2-1}}. \tag{A1}$$

We are interested in the $\Lambda \to \infty$, $\epsilon = 1-a-b \to 0$ limit of (A1). The limit $\epsilon \to 0$ of the second integral can be taken directly, after which the integral can be expressed in terms of elementary function. In taking the limit $\Lambda \to \infty$, we only need to keep up to constant terms

$$\begin{aligned}&\lim_{\epsilon\to 0,\Lambda\to\infty}\int_1^\Lambda \frac{ds}{\sqrt{s^2-1}}\left(\frac{s-a-b}{s-a+b}\right)^{1/2}\\ &= \lim_{\Lambda\to\infty}\int_1^\Lambda ds\left(\frac{1}{(s+1)(s-1+2b)}\right)^{1/2}\\ &= 2\ln 2 - 2\ln(\sqrt{2}+\sqrt{2b}) + \ln\Lambda + O(\Lambda^{-1}).\end{aligned} \tag{A2}$$

The third term is done in a similar way:

$$\lim_{\Lambda\to\infty}\int_1^\Lambda \frac{ds}{\sqrt{s^2-1}} = \ln 2 + \ln\Lambda + O(\Lambda^{-1}). \tag{A3}$$

The evaluation of the first term needs some effort. The first term can be expressed in terms of elliptic integrals. The formal expression is not very helpful in obtaining asymptotics. We instead use the following representation,

$$\begin{aligned}&\int_1^\Lambda \frac{ds}{\sqrt{s^2-1}}\left(\frac{s-a+b}{s-a-b}\right)^{1/2}\\ &= \frac{2}{\sqrt{(1-a+b)(1+a+b)}}\left[(1-a-b)\right.\\ &\quad\times\int_0^{\sin\nu}\frac{dx}{(1-\frac{2}{1+a+b}x^2)\sqrt{(1-x^2)(1-q^2x^2)}}\\ &\quad\left.+2b\int_0^{\sin\nu}\frac{dx}{\sqrt{(1-x^2)(1-q^2x^2)}}\right],\end{aligned}$$

where

$$\sin\nu = \left(\frac{(1+a+b)(\Lambda-1)}{2(\Lambda-a-b)}\right)^{1/2},$$
$$q^2 = \frac{4b}{(1-a+b)(1+a+b)}. \tag{A4}$$

We first look at the second integral in (A4). Expanding the denominator of the integrand, we obtain

$$\sqrt{(1-x^2)(1-q^2x^2)} = \sqrt{\lambda\left(\lambda-\frac{1}{2}+\frac{1}{2b}\right)}\epsilon + O(\epsilon^2), \tag{A5}$$

where $x^2 = 1-\epsilon\lambda$. The upper bound of x, in the limit $\epsilon \to 0$, is given by

$$\sin\nu = 1 - \frac{\epsilon}{4}\frac{\Lambda+1}{\Lambda-1} + O(\epsilon^2), \tag{A6}$$

which translates to the lower bound of λ: $\lambda \geq \frac{1}{2}\frac{\Lambda+1}{\Lambda-1}$. Assuming that the integral up to constant terms arises from the region $\lambda \sim O(1)$ or $1-x \sim O(\epsilon)$, we obtain the result for the integral

$$\frac{\epsilon}{2}\int_{\frac{1}{2}\frac{\Lambda+1}{\Lambda-1}}^{\lambda_s} d\lambda \frac{1}{\sqrt{\lambda(\lambda-\frac{1}{2}+\frac{1}{2b})\epsilon}} = 2\ln 2 - \ln\left(\sqrt{2}+\sqrt{\frac{2}{b}}\right) + \frac{1}{2}\ln\lambda_s, \tag{A7}$$

where $\lambda_s \sim O(1)$ is the cutoff of the integral. We note that there is a logarithmic divergence in λ_s, which means that there must be a contribution from region $1-x \gg O(\epsilon)$ to cancel the divergence. We evaluate the other contribution below,

$$\int_0^{\sqrt{1-\epsilon\lambda_s}} \frac{dx}{\sqrt{(1-x^2)(1-q^2x^2)}} = \frac{1}{2}\left(-\ln\frac{\epsilon}{4} - \ln\lambda_s\right) + O(\lambda_s^{-1}). \tag{A8}$$

The logarithmic divergences indeed cancel upon adding (A7)–(A8). The term $O(\lambda_s^{-1})$ can be ignored when we take $1 \ll \lambda_s \ll O(1/\epsilon)$. There is also a $\ln\epsilon$ divergence term, which can be traced back to light cone singularity integrated over spatial coordinate. This term is canceled by the zero temperature counterpart. The evaluation of the other integral follows similar procedure. We expand the denominator of the integrand as

$$\left(1-\frac{2}{1+a+b}x^2\right)\sqrt{(1-x^2)(1-q^2x^2)} = \left(\lambda-\frac{1}{2}\right)\sqrt{\lambda}\sqrt{\lambda-\frac{1}{2}+\frac{1}{2b}}\epsilon^2 + O(\epsilon^3). \tag{A9}$$

The integration from region $1-x \sim O(\epsilon)$ gives

$$\lim_{\Lambda\to\infty}\frac{\epsilon}{2}\int_{\frac{1}{2}\frac{\Lambda+1}{\Lambda-1}}^{\lambda_s}\frac{1}{(\lambda-\frac{1}{2})\sqrt{\lambda}\sqrt{\lambda-\frac{1}{2}+\frac{1}{2b}}\epsilon^2} = \frac{-2\sqrt{b}\tanh^{-1}(\sqrt{b}) + \sqrt{b}(\ln 2 - \ln(1-b) + \ln\Lambda)}{\epsilon}. \tag{A10}$$

We do not see a dependence on the cutoff λ_s, suggesting that we can take $\lambda_s \to \infty$ safely. Adding (A7)–(A8) and (A10), we obtain the final result for (A4) in the limit $\epsilon \to 0$, $\Lambda \to \infty$:

$$-2\tanh^{-1}\sqrt{b} + 6\sqrt{b}\ln 2 - 2\sqrt{b}\ln\left(\sqrt{2}+\sqrt{\frac{2}{b}}\right) - \sqrt{b}\ln\epsilon - \ln\frac{1-b}{2\Lambda}. \tag{A11}$$

As remarked before, the $\ln\Lambda$ term will be canceled by (A2)–(A3) and the $\ln\epsilon$ term will be canceled by the zero temperature counterpart.

[1] J. Aparicio and E. Lopez, Evolution of two-point functions from holography, J. High Energy Phys. 12 (2011) 082.

[2] R. Baier, S. A. Stricker, O. Taanila, and A. Vuorinen, Holographic dilepton production in a thermalizing plasma, J. High Energy Phys. 07 (2012) 094.

[3] Rudolf Baier, S. A. Stricker, Olli Taanila, and A. Vuorinen, Production of prompt photons: holographic duality and thermalization, Phys. Rev. D **86**, 081901 (2012).

[4] V. Balasubramanian, A. Bernamonti, B. Craps, V. Keränen, E. Keski-Vakkuri, B. Müller, L. Thorlacius, and J. Vanhoof, Thermalization of the spectral function in strongly coupled two-dimensional conformal field theories, J. High Energy Phys. 04 (2013) 069.

[5] V. Balasubramanian, A. Bernamonti, J. de Boer, N. Copland, B. Craps, E. Keski-Vakkuri, B. Muller, A. Schafer, M. Shigemori, and W. Staessens, Holographic thermalization, Phys. Rev. D **84**, 026010 (2011).

[6] V. Balasubramanian, A. Bernamonti, J. de Boer, N. Copland, B. Craps, E. Keski-Vakkuri, B. Muller, A. Schafer, M. Shigemori, and W. Staessens, Thermalization of Strongly Coupled Field Theories, Phys. Rev. Lett. **106**, 191601 (2011).

[7] V. Balasubramanian, A. Bernamonti, J. de Boer, B. Craps, L. Franti, F. Galli, E. Keski-Vakkuri, B. Müller, and A. Schäfer, Inhomogeneous holographic thermalization, J. High Energy Phys. 10 (2013) 082.

[8] V. Balasubramanian, A. Bernamonti, J. de Boer, B. Craps, L. Franti, F. Galli, E. Keski-Vakkuri, B. Müller, and A. Schäfer, Inhomogeneous Thermalization in Strongly Coupled Field Theories, Phys. Rev. Lett. **111**, 231602 (2013).

[9] H. Bantilan, F. Pretorius, and S. S. Gubser, Simulation of asymptotically AdS5 spacetimes with a generalized harmonic evolution scheme, Phys. Rev. D **85**, 084038 (2012).
[10] W. Baron, D. Galante, and M. Schvellinger, Dynamics of holographic thermalization, J. High Energy Phys. 03 (2013) 070.
[11] G. Beuf, M. P. Heller, R. A. Janik, and R. Peschanski, Boost-invariant early time dynamics from AdS/CFT, J. High Energy Phys. 10 (2009) 043.
[12] S. Bhattacharyya and S. Minwalla, Weak field black hole formation in asymptotically AdS spacetimes, J. High Energy Phys. 09 (2009) 034.
[13] E. Caceres and A. Kundu, Holographic thermalization with chemical potential, J. High Energy Phys. 09 (2012) 055.
[14] E. Caceres, A. Kundu, J. F. Pedraza, and D.-L. Yang, Weak field collapse in AdS: introducing a charge density, J. High Energy Phys. 06 (2015) 111.
[15] P. Calabrese and J. L. Cardy, Time Dependence of Correlation functions Following a Quantum Quench, Phys. Rev. Lett. **96**, 136801 (2006).
[16] S. Caron-Huot, P. M. Chesler, and D. Teaney, Fluctuation, dissipation, and thermalization in nonequilibrium AdS5 black hole geometries, Phys. Rev. D **84**, 026012 (2011).
[17] J. Casalderrey-Solana, M. P. Heller, D. Mateos, and W. van der Schee, From Full Stopping to Transparency in a Holographic Model of Heavy Ion Collisions, Phys. Rev. Lett. **111**, 181601 (2013).
[18] P. M. Chesler and D. Teaney, Dynamical Hawking radiation and holographic thermalization (2011).
[19] P. M. Chesler and D. Teaney, Dilaton emission and absorption from far-from-equilibrium non-Abelian plasma (2012).
[20] P. M. Chesler and L. G. Yaffe, Horizon Formation and Far-from-Equilibrium Isotropization in Supersymmetric Yang-Mills Plasma, Phys. Rev. Lett. **102**, 211601 (2009).
[21] P. M. Chesler and L. G. Yaffe, Boost-invariant flow, black hole formation, and far-from-equilibrium dynamics in $N = 4$ supersymmetric Yang-Mills theory, Phys. Rev. D **82**, 026006 (2010).
[22] P. M. Chesler and L. G. Yaffe, Holography and Colliding Gravitational Shock Waves in Asymptotically AdS5 Spacetime, Phys. Rev. Lett. **106**, 021601 (2011).
[23] P. M. Chesler and L. G. Yaffe, Numerical solution of gravitational dynamics in asymptotically anti–de Sitter spacetimes, J. High Energy Phys. 07 (2014) 086.
[24] P. M. Chesler and L. G. Yaffe, Holography and off-center collisions of localized shock waves, J. High Energy Phys. 10 (2015) 070.
[25] U. H. Danielsson, E. Keski-Vakkuri, and M. Kruczenski, Spherically collapsing matter in AdS, holography, and shellons, Nucl. Phys. **B563**, 279 (1999).
[26] U. H. Danielsson, E. Keski-Vakkuri, and M. Kruczenski, Black hole formation in AdS and thermalization on the boundary, J. High Energy Phys. 02 (2000) 039.
[27] J. R. David and S. Khetrapal, Thermalization of Green functions and quasinormal modes, J. High Energy Phys. 07 (2015) 041.
[28] E. D'Hoker and D. Z. Freedman, in *Strings, Branes, and Extra Dimensions: TASI 2001: Proceedings* (World Scientific, Boulder, 2002), p. 3–158.
[29] H. Ebrahim and M. Headrick, Instantaneous thermalization in holographic plasmas (2010).
[30] J. Erdmenger, C. Hoyos, and S. Lin, Time singularities of correlators from Dirichlet conditions in AdS/CFT, J. High Energy Phys. 03 (2012) 085.
[31] J. Erdmenger and S. Lin, Thermalization from gauge/gravity duality: evolution of singularities in unequal time correlators, J. High Energy Phys. 10 (2012) 028.
[32] J. Erdmenger, S. Lin, and T. H. Ngo, A moving mirror in AdS space as a toy model for holographic thermalization, J. High Energy Phys. 04 (2011) 035.
[33] D. Galante and M. Schvellinger, Thermalization with a chemical potential from AdS spaces, J. High Energy Phys. 07 (2012) 096.
[34] D. Garfinkle and L. A. P. Zayas, Rapid thermalization in field theory from gravitational collapse, Phys. Rev. D **84**, 066006 (2011).
[35] D. Garfinkle, L. A. P. Zayas, and D. Reichmann, On field theory thermalization from gravitational collapse, J. High Energy Phys. 02 (2012) 119.
[36] S. B. Giddings and A. Nudelman, Gravitational collapse and its boundary description in AdS, J. High Energy Phys. 02 (2002) 003.
[37] D. Grumiller and P. Romatschke, On the collision of two shock waves in AdS(5), J. High Energy Phys. 08 (2008) 027.
[38] M. P. Heller, R. A. Janik, and P. Witaszczyk, The Characteristics of Thermalization of Boost-Invariant Plasma from Holography, Phys. Rev. Lett. **108**, 201602 (2012).
[39] V. E. Hubeny, H. Liu, and M. Rangamani, Bulk-cone singularities and signatures of horizon formation in AdS/CFT, J. High Energy Phys. 01 (2007) 009.
[40] J. Järvelä, V. Keränen, and E. Keski-Vakkuri, Conformal quantum mechanics and holographic quench (2015).
[41] V. Keranen and P. Kleinert, Nonequilibrium scalar two point functions in AdS/CFT, J. High Energy Phys. 04 (2015) 119.
[42] S. Lin and E. Shuryak, Toward the AdS/CFT gravity dual for high energy collisions. 3. Gravitationally collapsing shell and quasiequilibrium, Phys. Rev. D **78**, 125018 (2008).
[43] P. Romatschke and J. D. Hogg, Preequilibrium radial flow from central shock-wave collisions in AdS5, J. High Energy Phys. 04 (2013) 048.
[44] K. Skenderis and B. C. van Rees, Real-Time Gauge/Gravity Duality, Phys. Rev. Lett. **101**, 081601 (2008).
[45] K. Skenderis and B. C. van Rees, Real-time gauge/gravity duality: prescription, renormalization, and examples, J. High Energy Phys. 05 (2009) 085.
[46] D. Steineder, S. A. Stricker, and A. Vuorinen, Holographic Thermalization at Intermediate Coupling, Phys. Rev. Lett. **110**, 101601 (2013).
[47] D. Steineder, S. A. Stricker, and A. Vuorinen, Probing the pattern of holographic thermalization with photons, J. High Energy Phys. 07 (2013) 014.
[48] W. van der Schee, P. Romatschke, and S. Pratt, Fully Dynamical Simulation of Central Nuclear Collisions, Phys. Rev. Lett. **111**, 222302 (2013).
[49] B. Wu and P. Romatschke, Shock-wave collisions in AdS5: approximate numerical solutions, Int. J. Mod. Phys. C **22**, 1317 (2011).